Supplementary Table 1: Coverage depth of Exome-Seq, RNA-Seq, and Whole Genome Sequencing

	Exome Sequencing	RNA-Seq	Whole Genome Sequencing
Sample	Coverage Depth	Millions of Unique Mapped Reads	Coverage Depth
1	212.296	-	-
2	229.655	79.41	-
3	221.612	-	-
4	191.248	-	-
5	237.056	-	-
6	159.702	119.08	-
7	232.187	-	-
8	206.878	-	-
9	238.57	28.76	-
10	176.488	-	-
11	200.226	-	-
12	225.346	188.08	-
13	148.801	194.55	33.97
14	333.623	-	-
15	207.053	86.94	-
16	256.855	-	-
17	212.514	200.65	32.13
18	228.644	-	-
19	142.219	93.12	-
20	251.65	-	-
21	219.13	-	-
22	211.489	-	-
23	313.064	-	-
24	235.35	-	-
25	230.113	-	-
26	277.415	86.38	-
27	187.807	-	-
28	256.855	-	-
29	227.849	-	-
30	185.597	-	-
31	220.994	-	-
32	152.91	76.53	-
33	257.772	-	-
34	209.109	-	-
35	307.703	42.41	-
36	168.945	-	-
37	236.272	-	-
38	190.454	-	-
39	202.544	-	-
40	169.274	-	-

Supplementary Table 2. C>T mutations in ECP-naïve and ECP-experienced patients.

ECP status	Total # SSNVs	Total # C>T SSNVs	% C>T dipyrimidine	% C>T non-dipyrimidine
ECP-neg (n = 3)	127	83	80	20
ECP-pos (n = 37)	2,722	1,933	76	24

ECP-neg, ECP-naïve; ECP-pos, ECP-experienced.

Supplementary Table 3a. Concordance of calls between exome sequencing and WGS (n=2)

Number of exome somatic variants with >10 coverage in WGS	120
Number of exome somatic variants with mutant base in WGS	119
% concordance of somatic variants between exome sequencing and WGS	99.4%

Table 3b. Concordance of calls between exome sequencing and RNA-seq (n=11)

Number of exome somatic variants with >20x coverage in RNA-seq	192
Number of exome somatic variants with mutant base in RNA-seq	184
% concordance of somatic variants between exome sequencing and RNA-seq	96%

Supplementary Table 4. SCNVs confirmed by whole genome sequencing.

SCNVs identified by exome sequencing	43
SCNVs identified by WGS and Patchwork-R	41
SCNVs identified by WGS and Breakdancer	1

Supplementary Table 5. Read counts supporting SSNVs in putative driver genes in CTCL.

Sample	Tumor Purity	Gene	AA change	Position (hg18)	CTCL			Monocyte		
					Ref cov	Nonref cov	MAF	Ref cov	Nonref cov	MAF
19	93.40%	*ARID1A*	N1705fs	chr1:26,974,774	118	53	31%	300	1	0.3%
15	99.70%	*ARID1A*	Q1454X	chr1:26,973,665	49	53	52%	113	0	0.0%
14	95.00%	*ATM*	G2694A	chr11:107,710,976	21	203	91%	170	1	0.6%
13	99.30%	*BRAF*	D594N	chr7:140,099,624	197	72	27%	283	1	0.4%
5	99.80%	*CD28*	Q77P	chr2: 204,299,778	179	140	44%	287	0	0.0%
5	99.80%	*CD28*	K81N	chr2:204,299,791	179	140	44%	287	0	0.0%
14	95.00%	*CD28*	F51V	chr2:204,299,699	177	149	46%	137	1	0.7%
10	99.60%	*CD28*	F51I	chr2:204,299,699	74	82	53%	202	2	1.0%
11	99.00%	*CDKN2A*	W15X	chr9:21,964,783	0	10	100%	14	1	6.7%
12	99.70%	*CTCF*	L309V	chr16:66,203,498	141	87	38%	256	0	0.0%
32	99.00%	*DNMT3A*	P777L	chr2:25,315,581	115	86	43%	224	6	2.6%
32	99.00%	*DNMT3A*	S669F	chr2:25,318,011	72	75	51%	198	5	2.5%
11	99.00%	*DNMT3A*	Y584X	chr2:25,320,627	0	35	100%	52	2	3.7%
30	97.80%	*DNMT3A*	P233L	chr2:25,324,567	55	25	31%	93	1	1.1%
5	99.80%	*FAS*	E261K	chr10:90,763,960	111	177	61%	392	0	0.0%
13	99.30%	*FAS*	D265E	chr10:90,763,974	3	85	97%	259	0	0.0%
8	99.60%	*FAS*	S212C	chr10:90,761,802	10	125	93%	273	0	0.0%
32	99.00%	*IRF4*	F358I	chr6:346,753	64	35	35%	98	0	0.0%
11	99.00%	*IRF4*	F359L	chr6:346,755	67	34	34%	97	5	4.9%
37	99.60%	*NFKB2*	SS*	chr10:104,150,692	53	30	36%	41	0	0.0%
7	97.60%	*PLCG1*	E1163K	chr20:39,235,798	125	60	32%	170	1	0.6%
6	99.60%	*PLCG1*	D342N	chr20:39,225,988	103	104	50%	165	1	0.6%
14	95.00%	*PLCG1*	R48W	chr20:39,199,837	41	37	47%	45	2	4.3%
3	96.00%	*PLCG1*	S345F	chr20:39,225,998	118	87	42%	191	0	0.0%
33	97.00%	*RHOA*	N117I	chr3:49,374,991	173	157	48%	153	1	0.6%
13	99.30%	*RHOA*	N117I	chr3:49,374,991	124	128	51%	212	4	1.9%
4	99.20%	*RHOA*	R70K	chr3:49,380,933	146	114	44%	150	0	0.0%
21	97.60%	*STAT5B*	N642H	chr17:37,613,255	149	119	44%	198	5	2.5%
32	99.00%	*TP53*	R273P	chr17:7,517,845	48	131	73%	280	4	1.4%

25	99.10%	*TP53*	A215V	chr17:7,514,712	11	81	88%	80	14	14.9%
24	98.30%	*TP53*	R196X	chr17:7,518,988	3	199	99%	211	5	2.3%
11	99.00%	*TP53*	S94X	chr17:7,520,131	1	50	98%	177	1	0.6%
20	100.00%	*TP53*	T155N	chr17:7,519,191	6	97	94%	90	10	10.0%
40	100.00%	*TP53*	I254T	chr17:7,518,245	0	45	100%	68	8	10.5%
4	99.20%	*TP53*	S34X	chr17:7,519,158	5	47	90%	67	0	0.0%
2	97.70%	*ZEB1*	Q855X	chr10:31,850,829	8	74	90%	212	0	0.0%
37	99.60%	*ZEB1*	Q538X	chr10:31,849,929	74	103	58%	65	0	0.0%
31	97.50%	*ZEB1*	Y251C	chr10:31,843,604	156	238	60%	278	30	9.7%

Ref Cov; number of reads of reference allele, Nonref Cov, number of reads of non-reference allele; MAF, minor allele frequency.

*Splice-site mutation upstream of exon 17.

Supplementary Table 6. SSNVs in CTCL identified in other cancers

Gene	Mutations	Other Cancers
BRAF	D594N	Melanoma**
CD28	F51V	AITL
CARD11	M360K	DLBCL
CDKN2A	W15X	HNSCC
DNMT3A	S669F	Lung
FAS	E261K	Lung
	D265E	DLBCL
STAT5B	N642H	T-LGL**
TP53	R273P	Breast
	A215V	CNS
	R196X	Breast
	S94X	Esophagus
	T155N	Lung
	I254T	Colon
	S34X	Lung

Other cancer, cancer previously described to be harboring identical somatic SNV. AITL, angioimmunoblastic T-cell lymphoma; CNS, central nervous system; DLBCL, diffuse large B-cell lymphoma; HNSCC, head and neck squamous cell carcinoma; T-LGL, T- cell large granular lymphocytic leukemia. **functionally validated to be a gain-of-function mutation.

Supplementary Table 7. Significant Focal Deletions

Cytoband	Q-Value	Residual Q-Value	Wide Peak Boundaries	% of CTCLs With Deletions‡			# Genes in Peak	Candidate Gene	GRAIL P-value
				Total	Focal	Broad			
1p36.11	$6.59x10^{-16}$	$6.59x10^{-16}$	chr1:26,673,679–27,110,886	57.5%	57.5%	0.0%	7	***ARID1A****	-
9p21.3	$6.59x10^{-16}$	$6.59x10^{-16}$	chr9:21,849,450–21,996,041	40.0%	37.5%	2.5%	1	***CDKN2A****	-
10p11.22	$4.57x10^{-14}$	$2.01x10^{-13}$	chr10:31,205,853–32,136,797	60.0%	32.5%	27.5%	1	***ZEB1***	-
10q24.32	$1.74x10^{-8}$	$4.77x10^{-7}$	chr10:104,131,016–104,230,563	67.5%	42.5%	25.0%	7	***NFKB2***	-
2p23.3	$5.57x10^{-7}$	$5.57x10^{-7}$	chr2:24,949,121–25,818,354	37.5%	30.0%	7.5%	4	***DNMT3A****	-
11q22.3	$1.69x10^{-5}$	$1.76x10^{-5}$	chr11:107,234,547–107,759,139	30.0%	22.5%	7.5%	5	ATM*	-
2q37.3	0.00010519	0.00010354	chr2:239,018,134–242,951,149	20.0%	20.0%	0.0%	38	PDCD1	0.0035
19p13.3	$1.19x10^{-7}$	0.00039797	chr19:1–55,701,376	42.5%	42.5%	0.0%	1078	STK11**	-
9q21.32	$2.94x10^{-5}$	0.00048049	chr9:80,386,282–90,795,694	32.5%	17.5%	15.0%	33	DAPK1	0.00062
13q14.2	0.00057769	0.00056364	chr13:47,731,103–56,619,937	30.0%	20.0%	10.0%	40	RB1*	-
19p13.3	$1.35x10^{-7}$	0.000581	chr19:2,029,483–3,927,502	32.5%	32.5%	0.0%	53	GADD45B	0.025
12p13.2	0.00088263	0.00085553	chr12:9,777,007–14,468,100	17.5%	17.5%	0.0%	64	CDKN1B*	-
6q23.3	$1.76x10^{-5}$	0.0016017	chr6:138,243,081–138,525,040	25.0%	25.0%	0.0%	2	TNFAIP3***	-
10q21.2	0.00018739	0.00236	chr10:63,698,286–64,053,033	52.5%	17.5%	35.0%	2	ZNF365	0.58
10q26.3	0.00010236	0.004758	chr10:127,512,506–135,374,737	55.0%	35.0%	20.0%	46	MGMT	0.00016
7p21.1	0.011766	0.011766	chr7:15,566,451–36,519,345	27.5%	22.5%	5.0%	107	NFE2L3*	-
9q31.1	0.00078864	0.022893	chr9:96,260,592–105,897,449	25.0%	20.0%	5.0%	58	XPA	0.39
6q25.2	0.00078369	0.04894	chr6:153,645,511–170,899,992	20.0%	20.0%	0.0%	73	CCR6	0.12
12q21.33	0.048579	0.04894	chr12:87,113,009–111,341,205	20.0%	17.5%	2.5%	160	SOCS2	0.076
6q21	0.052955	0.051525	chr6:106,661,861–112,488,015	17.5%	15.0%	2.5%	42	TRAF3IP2	0.02
16q22.1	0.056991	0.055785	chr16:66,074,546–66,236,753	15.0%	15.0%	0.0%	2	CTCF*	-
10q26.11	0.00030478	0.095529	chr10:120,779,987–124,142,656	55.0%	35.0%	20.0%	19	BAG3	0.46
10q23.31	0.015023	0.11663	chr10:90,763,175–90,964,816	40.0%	12.5%	27.5%	2	***FAS***	-
11p13	0.11475	0.11663	chr11:31,441,250–35,596,790	20.0%	10.0%	10.0%	28	WT1*	-

6q25.1	0.00050411	0.1338	chr6:149,953,508–150,112,805	22.5%	22.5%	0.0%	3	LATS1	0.17
16q24.2	0.13018	0.1338	chr16:86,667,813–88,154,820	12.5%	12.5%	0.0%	21	BANP	0.021
13q12.13	0.13373	0.1338	chr13:1–40,031,653	17.5%	10.0%	7.5%	101	BRCA2**	-
1p22.1	0.15633	0.15669	chr1:71,317,019–96,960,088	15.0%	15.0%	0.0%	106	RPL5*	-
8p23.1	0.24317	0.23282	chr8:1–146,274,826	40.0%	20.0%	20.0%	644	EGR3**	-

Bold, Genes with statistically significant gene localizing data. * Putative tumor suppressors published by the TCGA to be significantly mutated across tumors of multiple lineage types[1]. **There are multiple consensus tumor suppressors in the GISTIC interval, the gene with the highest SCNV mutation rate is listed. ***_TNFAIP3_ was listed because it was recently implicated in leukemic CTCL[2]. The remaining candidate genes reflect the highest-scoring gene in the interval identified by GRAIL. GRAIL P-values are corrected for multiple hypothesis testing. ‡Only the focal SCNVs are listed for CTCL samples with both focal SCNVs and broad SCNVs involving the indicated GISTIC interval.

Supplementary Table 8. Significant Focal Amplifications

Cytoband	Q-value	Residual Q-value	Wide Peak Boundaries	% of CTCLs With Amplifications‡			# Genes in Peak	Candidate Gene	GRAIL P-value
				Total	Focal	Broad			
10p15.1	0.00029474	0.00029474	chr10:5,882,522–7,245,908	30.0%	17.5%	12.5%	9	PRKCQ	6.78×10^{-5}
10p12.33	0.063691	0.063691	chr10:15,250,463–18,469,816	22.5%	10.0%	12.5%	21	TRDMT1	0.18
7p22.2	0.098621	0.098621	chr7:1-4,248,090	22.5%	17.5%	5.0%	34	CARD11	0.00031
9p24.2	0.11963	0.11963	chr9:2,612,161–5,512,649	12.5%	12.5%	0.0%	20	JAK2	3.27×10^{-5}
6p25.3	0.21318	0.21318	chr6:1–1,258,328	5.0%	5.0%	0.0%	5	IRF4	0.0015
7q34	0.21318	0.21318	chr7:127,929,037–158,821,424	17.5%	10.0%	7.5%	222	***BRAF*****	-
17q11.2	0.21318	0.21318	chr17:21,750,215–37,983,285	62.5%	10.0%	52.5%	283	***STAT5B***	-

Bold, Genes with gene localizing data. * Putative oncogene published by the TCGA to be significantly mutated across tumors of multiple lineage types[1]. **There are multiple consensus oncogenes in the GISTIC interval, the gene with the highest SCNV mutation rate is listed. The remaining candidate genes reflect the highest-scoring gene in the interval identified by GRAIL. GRAIL P-values are corrected for multiple hypothesis testing. ‡Only the focal SCNVs are listed for CTCL samples with both focal SCNVs and broad SCNVs involving the indicated GISTIC interval.

Supplementary Table 9. Broad deletions in CTCL

Chromosome Arm	# CTCL Samples With Deletions	Q-value
1p	0	0.8992776
1q	0	0.8992776
2p	2	0.8992776
2q	0	0.8992776
3p	0	0.8992776
3q	0	0.8992776
4p	0	0.8992776
4q	0	0.8992776
5p	0	0.8992776
5q	0	0.8992776
6p	0	0.8992776
6q	1	0.8992776
7p	2	0.8992776
7q	0	0.8992776
8p**	9	0.000680835
8q	0	0.8992776
9p	3	0.7896044
9q	4	0.4562849
10p**	8	0.002859392
10q**	12	2.83×10^{-06}
11p	4	0.4562849
11q	3	0.7896044
12p	0	0.8992776
12q	1	0.8992776
13q	3	0.7896044
14q	0	0.8992776
15q	0	0.8992776
16p	0	0.8992776
16q	0	0.8992776
17p**	34	0
17q	0	0.8992776
18p	0	0.8992776
18q	0	0.8992776
19p	0	0.8992776
19q	0	0.8992776
20p	1	0.8992776
20q	0	0.8992776
21q	0	0.8992776
22q	0	0.8992776

* False discovery rate between 0.1 and 0.25.
** False discovery rate below 0.1

Supplementary Table 10. Broad amplifications in CTCL

Chromosome Arm	# CTCL Samples With Amplifications	Q-value
1p	0	0.9096584
1q	0	0.9096584
2p	0	0.9096584
2q	0	0.9096584
3p	0	0.9096584
3q	0	0.9096584
4p	4	0.3537442
4q**	6	0.07615465
5p	2	0.9096584
5q	1	0.9096584
6p	0	0.9096584
6q	0	0.9096584
7p	2	0.9096584
7q*	5	0.1336047
8p*	5	0.1336047
8q**	17	3.88×10^{-11}
9p	1	0.9096584
9q	1	0.9096584
10p*	5	0.1336047
10q	1	0.9096584
11p	0	0.9096584
11q	0	0.9096584
12p	0	0.9096584
12q	0	0.9096584
13q	1	0.9096584
14q	0	0.9096584
15q	0	0.9096584
16p	1	0.9096584
16q	0	0.9096584
17p	1	0.9096584
17q**	23	0
18p*	5	0.1336047
18q*	5	0.1336047
19p	0	0.9096584
19q	0	0.9096584
20p	1	0.9096584
20q	1	0.9096584
21q	3	0.7925349
22q	0	0.9096584

* False discovery rate between 0.1 and 0.25.
** False discovery rate below 0.1

Supplementary Table 11. Clonality of recurrent mutations in driver genes in CTCL

	SCNV		SSNV		Total	
Gene	**<75%**	**76-100%**	**<75%**	**76-100%**	**<75%**	**76-100%**
TP53	1	35	0	7	1	42
ZEB1	2	22	0	3	2	25
ARID1A	4	19	1	1	5	20
DNMT3A	3	12	1	3	4	15
CDKN2A	0	16	0	1	0	17
FAS	2	14	0	3	2	17
NFKB2	0	4	1	0	1	4
CD28	0	0	0	4	0	4
PLCG1	0	0	1	3	1	3
RHOA	0	0	0	3	0	3
STAT5B	5	20	0	1	5	21
BRAF	0	0	1	0	1	0

Each SCNV and SSNV was assessed for the % of tumor cells with the mutation. Samples were binned with <75% clonality and 75-100% clonality. Listed are numbers of samples with each SCNV and SSNV in each bin.

Supplementary Table 12. SCNVs and SSNVs of candidate driver genes residing on significant focal deletions.

Cytoband	GISTIC Residual Q Value	# Genes in Peak	Candidate Gene	GRAIL P value	% of CTCLs With Deletions				# of SSNVs
					Total	Biallelic	Focal	Broad	
1p36.11	$6.59x10^{-16}$	7	***ARID1A****	-	57.5%	0.0%	57.5%	0.0%	NS (1), FS(1)
9p21.3	$6.59x10^{-16}$	1	***CDKN2A****	-	40.0%	30.0%	7.5%	2.5%	NS (1)
10p11.22	$2.01x10^{-13}$	1	***ZEB1***	-	60.0%	12.5%	20.0%	27.5%	NS (2), MS (1)
10q24.32	$4.77x10^{-7}$	7	***NFKB2****	-	10.0%	5.0%	5.0%	0.0%	SS (1)
2p23.3	$5.57x10^{-7}$	4	***DNMT3A****	-	37.5%	2.5%	27.5%	7.5%	NS (1), MS (3)
11q22.3	$1.76x10^{-5}$	5	ATM*	-	30.0%	2.5%	20.0%	7.5%	MS (1)
2q37.3	0.00010354	38	PDCD1	0.0035	20.0%	5.0%	15.0%	0.0%	-
19p13.3	0.00039797	1078	STK11**	-	30.0%	0.0%	30.0%	0.0%	-
9q21.32	0.00048049	33	DAPK1	0.00062	25.0%	0.0%	12.5%	12.5%	-
13q14.2	0.00056364	40	RB1*	-	25.0%	0.0%	15.0%	10.0%	MS (1)
19p13.3	0.000581	53	GADD45B	0.025	27.5%	0.0%	27.5%	0.0%	-
12p13.2	0.00085553	64	CDKN1B*	-	15.0%	0.0%	15.0%	0.0%	-
6q23.3	0.0016017	2	TNFAIP3***		25.0%	2.5%	22.5%	0.0%	-
10q21.2	0.00236	2	ZNF365	0.58	50.0%	0.0%	15.0%	35.0%	-
10q26.3	0.004758	46	MGMT	0.00016	47.5%	0.0%	30.0%	17.5%	-
7p21.1	0.011766	107	NFE2L3*	-	15.0%	0.0%	10.0%	5.0%	-
9q31.1	0.022893	58	XPA	0.39	20.0%	0.0%	15.0%	5.0%	-
6q25.2	0.04894	73	CCR6	0.12	15.0%	0.0%	15.0%	0.0%	-
12q21.33	0.04894	160	SOCS2	0.076	15.0%	0.0%	12.5%	2.5%	-
6q21	0.051525	42	TRAF3IP2	0.02	12.5%	0.0%	10.0%	2.5%	-
16q22.1	0.055785	2	CTCF*	-	12.5%	0.0%	12.5%	0.0%	MS (1)
10q26.11	0.095529	19	BAG3	0.46	52.5%	0.0%	32.5%	20.0%	-
10q23.31	0.11663	2	***FAS***	-	40.0%	2.5%	10.0%	27.5%	MS (3)
11p13	0.11663	28	WT1*	-	17.5%	0.0%	7.5%	10.0%	-
6q25.1	0.1338	3	LATS1	0.17	22.5%	0.0%	22.5%	0.0%	-

16q24.2	0.1338	21	BANP	0.021	2.5%	0.0%	2.5%	0.0%	-
13q12.13	0.1338	101	BRCA2**	-	15.0%	0.0%	5.0%	10.0%	MS (1)
1p22.1	0.15669	106	RPL5*	-	10.0%	0.0%	10.0%	0.0%	-
8p23.1	0.23282	644	EGR3**	-	30.0%	0.0%	7.5%	22.5%	-

Bold, Genes with statistically significant gene localizing data. * Putative tumor suppressors published by the TCGA to be significantly mutated across tumors of multiple lineage types[1]. **There are multiple consensus tumor suppressors in the GISTIC interval, the gene with the highest SCNV mutation rate is listed. ***_TNFAIP3_ was listed because it was recently implicated in leukemic CTCL[2]. The remaining candidate genes were identified by GRAIL. GRAIL P-values are corrected for multiple hypothesis testing. [t] For NFKB2, only the truncating mutations are shown. NS, represents nonsense mutations; FS, frameshift mutations; MS, missense mutations; SS, splice site mutations.

Supplementary Table 13. SCNVs and SSNVs for candidate driver genes on significant focal amplifications

Cytoband	GISTIC Residual Q-value	# Genes in Peak	Candidate Gene	GRAIL P-value	% of CTCLs With Amplifications			# of SSNVS
					Total	Focal	Broad	
10p15.1	0.00029474	9	PRKCQ	6.78×10^{-5}	30.0%	17.5%	12.5%	-
10p12.33	0.063691	21	TRDMT1	0.18	22.5%	10.0%	12.5%	-
7p22.2	0.098621	34	CARD11	0.00031	22.5%	17.5%	5.0%	MS (3)[#]
9p24.2	0.11963	20	JAK2	3.27×10^{-5}	12.5%	12.5%	0.0%	-
6p25.3	0.21318	5	IRF4	0.0015	5.0%	5.0%	0.0%	MS (2)
7q34	0.21318	222	***BRAF*****	-	15.0%	2.5%	12.5%	MS (1)[#]
17q11.2	0.21318	283	***STAT5B***	-	62.5%	5.0%	57.5%	MS (1)[#]

Bold, Genes with gene localizing data.* Putative oncogene published by the TCGA to be significantly mutated across tumors of multiple lineage types[1]. **There are multiple consensus oncogenes in the GISTIC interval, the gene with the highest SCNV mutation rate is listed. The remaining candidate genes were identified by GRAIL. GRAIL P-values are corrected for multiple hypothesis testing. MS, missense mutations. [#]Missense mutations were previously reported in other cancers.

Supplementary Table 14a. SCNVs and SSNVs of putative driver genes residing on narrow, significant focal deletions intervals (<10 Genes in GISTIC interval).

Candidate Gene	# Genes Residing on GISTIC Peak	GISTIC Residual Q-value	# SSNVs	% of CTCLs with Deletions			% of CTCLs with SCNV or SSNV	GRAIL P-value
				Biallelic	Monoallelic			
					Focal	Broad		
ATM*	5	1.8×10^{-5}	1	2.5	20	7.5	30	-
TNFAIP3**	2	0.0016	0	2.5	22.5	0	25	-
CTCF*	2	0.056	1	0	12.5	0	15	-

Table 14b. SCNVs and SSNVs of putative driver genes residing on narrow, significant focal amplification intervals (<10 Genes in GISTIC interval).

Candidate Gene	# Genes Residing on GISTIC Peak	GISTIC Residual Q-value	# SSNVs	% of CTCLs with Amplifications		% of CTCLs with SCNV or SSNV	GRAIL P-value
				Focal	Broad		
PRKCQ	9	0.00029	0	17.5	12.5	30	6.8×10^{-5}
IRF4	5	0.21318	2	5	0	10	0.0015

*Genes with statistically significant mutations across multiple lineage types as published by the TCGA. ***TNFAIP3* was listed because it was recently implicated in leukemic CTCL[2]. The remaining candidate genes were identified by GRAIL.

Supplementary Table 15a. Transcript levels of driver genes for which there are at least 3 CTCLs with the normal diploid gene copy number and at least 3 CTCLs with deletions.

Gene	Number of Diploid CTCLs	Mean FPKM of Normal	Standard Error	Number of CTCLs with SCNVs	Mean FPKM of Mutant	Standard Error	P-value
ARID1A	5*	32.37	4.103	5	20.5	2.733	0.016
CTCF	8	30.55	1.393	3	23.43	2.911	0.042
TNFAIP3	8	268.6	73.39	3	59.9	23.93	0.012
ZEB1	6*	12.76	1.476	3**	5.095	1.27	0.024

Supplementary Table 15b. Transcript levels of driver genes for which there are at least 3 CTCLs with the normal diploid gene copy number and at least 3 CTCLs with amplifications.

Gene	Number of Diploid CTCLs	Mean FPKM of Normal	Standard Error	Number of CTCLs with SCNVs	Mean FPKM of Mutant	Standard Error	P-value
STAT5B	3	91.37	9.05	8	144	8.685	0.012

Diploid CTCLs, CTCLs with two copies of indicated gene. FPKM, fragments per kilobase per million reads. P-values were calculated by one-sided Mann-Whitney t-test. * 1 sample was excluded from diploid CTCLs because it harbored a nonsense mutation. ** 1 sample was excluded from CTCLs with SCNVs because it harbored a biallelic deletion.
ǂ 1 sample was excluded from diploid CTCLs because it harbored an intragenic deletion.

Supplementary Table 16. Identification by whole genome sequencing of breakpoints contributing to SCNVs in CTCL.

Sample	Breakpoint #1			Breakpoint #2			Structural Variant	Driver genes	Total Reads	Micro-homology	Non-templated
	Chr	Position	Location	Chr	Position	Location		affected	Supporting		Sequence
13	1	26,713,590	Intergenic	1	27,941,189	Intron of *FAM76A*	Deletion	*ARID1A*	18	1	
13	1	148,622,707	Intron of *RPRD2*	1	149,660,970	Intron of *POGZ*	Deletion		16	1	
13	1	224,379,591	Intergenic	1	233,378,232	Intron of *RBM34*	Deletion		23	1	
13	1	228,512,286	Intergenic	1	233,382,968	Intron of *RBM34*	Inversion		16	1	
13	2	11,943,988	Intergenic	2	86,138,204	Intron of *POLR1A*	Inversion		33	0	
13	2	12,448,066	Intron of *AK001558*	2	85,728,835	Intron of *USP39*	Inversion		28	3	
13	2	25,342,324	Intron of *DNMT3A*	11	101,668,436	Intergenic	Translocation	*DNMT3A*, *ATM*	22	1	
13	2	26,099,685	Intergenic	11	117,868,561	Intron of *MLL*	Translocation	*DNMT3A*, *ATM*	16	1	
13	3	171,780,269	Intron of *SLC7A14*	10	73,141,626	Intron of *CDH23*	Translocation		18	1	
13	3	176,284,784	Intron of *NAALADL2*	10	66,110,178	Intergenic	Translocation	*ZEB1*	15	9	
13	5	139,813,420	Intron of *ANKHD1*	11	117,857,758	Exon of *MLL*	Translocation		13	2	
13	5	139,985,062	Intergenic	11	117,860,771	Intron of *MLL*	Translocation		28	0	
13	9	21,818,243	Intron of *MTAP*	9	31,671,084	Intergenic	Inversion	*CDKN2A*	30		4
13	9	31,207,570	Intergenic	9	21,818,204	Intron of *MTAP*	Deletion		29		1
13	10	25,778,773	Intron of *GPR158*	3	175,371,776	Intron of *NLGN1*	Translocation	*ZEB1*	16		0
13	10	72,379,661	Intergenic	10	107,233,329	Intergenic	Deletion		8		2
13	10	73,204,904	Intron of *CDH23*	3	175,193,528	Intron of *NLGN1*	Translocation		23	0	
13	10	73,309,035	Intergenic	10	57,650,001	Intergenic	Inversion		21	0	
13	10	89,295,708	Intron of *MINPP1*	10	90,907,696	Intergenic	Deletion	*FAS*	25		1
13	10	98,565,242	Intergenic	10	25,538,394	Intron of *GPR158*	Deletion		17		1
13	10	108,330,062	Intron of *SORCS1*	10	25,550,092	Exon of *GPR158*	Inversion		19		2
13	10	110,861,244	Intergenic	10	57,822,392	Intergenic	Inversion		16	3	
13	10	119,033,460	Exon of *PDZD8*	10	42,411,948	Intron of *ZNF338*	Deletion		33	1	
13	10	119,267,885	Intron of *EMX2OS*	10	56,596,808	Intron of *PCDH15*	Inversion		27	2	
17	2	24,367,403	intron of *ITSN2*	2	25,537,807	Intron of *DTNB*	Deletion	*DNMT3A*	19	5	

17	2	197,673,437	Intron of *ANKRD44*	2	199,342,112	Intergenic	Inversion		19	0	
17	2	198,522,274	intron of *PLCL1*	2	199,414,606	Intergenic	Deletion		25	2	
17	10	24,938,888	Intergenic	10	129,541,310	Intron of *ARHGAP21*	Deletion	*ZEB1*, *FAS*	11	2	
17	10	30,991,190	Intergenic	15	72,750,546	Intron of *EDC3*	Translocation	*ZEB1*	16		1
17	10	32,144,341	Intron of *ARHGAP12*	15	73,749,197	Intergenic	Translocation	*ZEB1*	10	1	
17	10	35,838,582	Intron of *CCNY*	11	30,352,778	Intergenic	Translocation		20	15	
17	10	57,379,788	Intergenic	10	59,091,465	Intergenic	Deletion		18	9	
17	10	57,380,995	Intergenic	10	129,415,540	Intergenic	Deletion		29	0	
17	10	60,008,131	Intron of *BICC1*	10	128,178,240	intron of *C10orf90*	Inversion		23	1	
17	10	65,707,339	Intergenic	10	60,337,921	Intergenic	Translocation		27	0	
17	10	103,775,255	Intron of *C10orf76*	10	104,566,246	Intron of *C10orf26*	Deletion	*NFKB2*	23	1	
17	10	104,150,525	Exon of *NFKB2*	5	92,742,617	Intergenic	Translocation	*NFKB2*	21	3	
17	10	104,165,993	Intron of *PSD*	5	87,323,821	Intergenic	Translocation	*NFKB2*	11	0	
17	10	121,408,863	Intron of *BAG3*	19	43,536,117	Intron of *C19orf15*	Translocation		8	1	
17	10	121,501,394	Intron of *INPP5F*	19	44,184,624	Intergenic	Translocation		25		2
17	10	128,122,034	Intron of *C10orf90*	10	57,882,148	Intergenic	Inversion		18	4	
17	10	128,777,367	Intron of *DOCK1*	12	18,904,702	Intergenic	Translocation		20	1	
17	10	130,061,878	Intergenic	10	65,535,231	Intergenic	Inversion		21		1
17	11	26,374,469	Intron of *ANO3*	11	30,033,694	Intergenic	Deletion		11		1
17	11	63,402,680	Intron of *MARK2*	10	34,676,505	Intron of *PARD3*	Translocation		15		4
17	12	17,974,225	Intergenic	12	25,562,201	Intron of *LMNTD1*	Inversion		31	3	
17	12	60,257,721	Intergenic	12	121,277,149	Exon of *DIABLO*	Inversion		14	2	
17	12	121,329,259	Intron of *CLIP1*	12	57,264,550	Intergenic	Translocation		17	0	
17	16	66,130,715	Intron of *FAM65A*	19	44,085,041	Intron of *NFKBIB*	Translocation	*CTCF*	24	1	
17	16	66,227,930	Intron of *CTCF*	1	23,836,991	Intron of *MDS2*	Translocation	*CTCF*	18	1	
17	17	7,211,140	Intergenic	17	7,849,358	Intron of *GUCY2D*	Deletion	*TP53*	17	8	

Supplementary Table 17. IL-2 primer sequences

Primer name	Target gene	Primer sequence
IL-2-FWD	IL-2	5’- CAAACCTCTGGAGGAAGTGC-3’
IL-2-REV	IL-2	5’- GGTTGCTGTCTCATCAGCAT-3’

References for supplementary tables:

1. Kandoth, C. *et al.* Mutational landscape and significance across 12 major cancer types. *Nature* **502**, 333-9 (2013).
2. Braun, F.C. *et al.* Tumor suppressor TNFAIP3 (A20) is frequently deleted in Sezary syndrome. *Leukemia* **25**, 1494-501 (2011).

Supplementary Figure 1. Cell surface staining of tumor cells and normal cells after flow cytometry activated cell sorting.

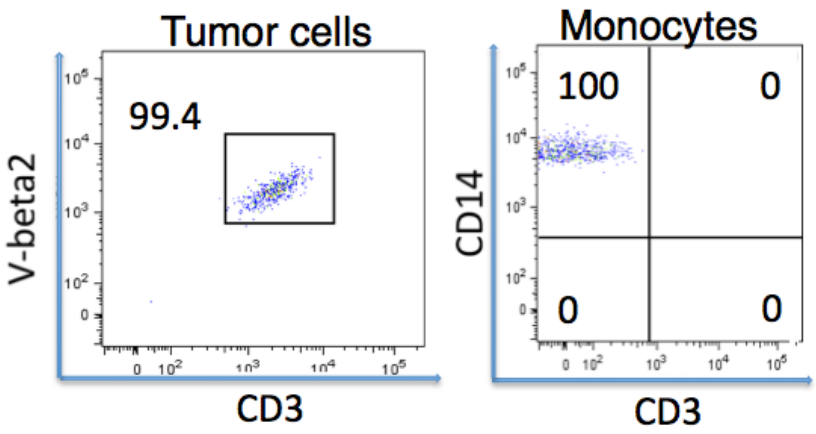

Flow cytometry activated cell sorting was performed to isolate CTCL cells and matched monocytes. The post-sort flow cytometry to assess uniformity of cell sorting is shown above. CTCL clones were identified by a T cell marker (CD3) and an antibody targeting the TCR V-β utilized by the leukemic CTCL clone (in this case, TCR-Vβ2). Monocytes were identified by the presence of CD14, a monocyte-specific marker, and the absence of CD3 staining.

Supplementary Figure 2. Somatic copy number mutations identified by relative coverage depth and changes in B-allele frequency (BAF) at informative SNPs

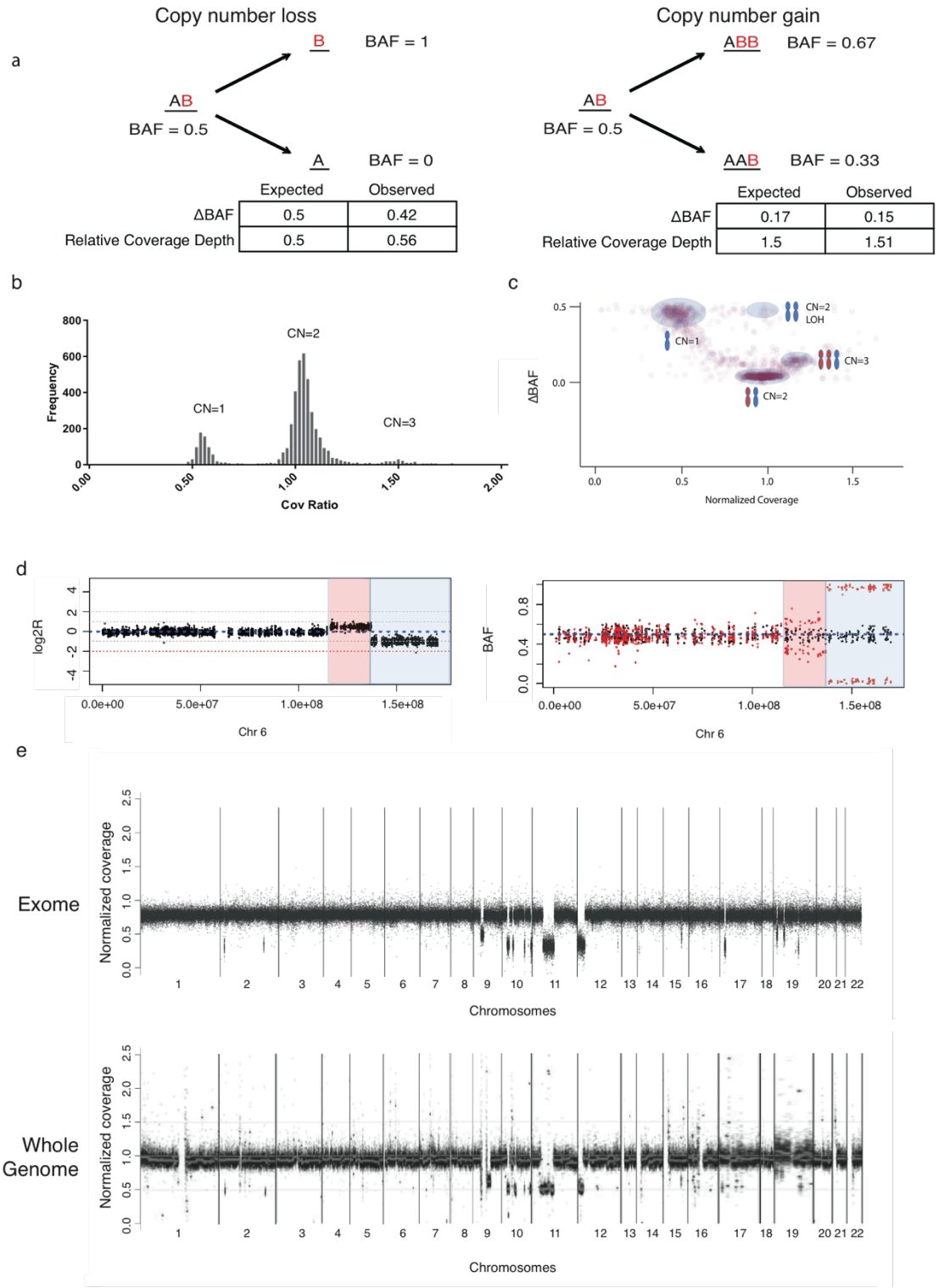

(a) Expected and observed changes in normalized coverage depth and B-allele frequency in copy number deletions and copy number gains identified by exome sequencing. **(b)** Histogram of normalized coverage depth of 50 kb segments in a sample of CTCL. The genome was binned into contiguous 50 kb segments. The normalized coverage depth from exome sequencing was calculated from the tumor: normal read depth of the segment compared to the average tumor:normal read depth across the genome. **(c)** Plots of B-allele frequency (BAF) vs. normalized read coverage generated by exome sequencing of all 40 samples. Copy number loss is marked by loss-of-heterozygosity (ΔBAF=0.5) and halving of normalized coverage. Copy neutral loss-of-heterozygosity is marked by loss-of-heterozygosity and no change in coverage depth. Copy number amplification is marked by characteristics changes in B-allele-frequency (ΔBAF=0.16) and increases in coverage depth. Each point represents one segment from one sample of a defined copy number. **(d)** A representative example of a plot of relative coverage depth and corresponding plot of BAF. Each point represents the $\log_2$ relative ratio (log2R) of coverage between tumor and normal sample at a targeted region from the Nimblegen array. The blue dotted line indicates an LRR of 0. The red dotted line indicates an LRR of –2. For the BAF plot, heterozygous SNVs in the normal (B-allele frequency of 0.4–0.6) are plotted in black. The BAFs of the tumors at the corresponding SNVs are plotted in red. An area designated as a copy number gain from 2->3 is shaded red. An area designated as a copy number loss from 2->1 is shaded blue. **(e)** Plots of normalized coverage generated by exome sequencing and whole genome sequencing. WGS plots were generated with Patchwork-R.

Supplementary Figure 3. Sanger sequencing of select point mutations.

(a) Representative chromatograms of Sanger DNA sequence of CTCL DNA for point mutations in *CD28* and *RHOA*. **(b)** Representative chromatograms of Sanger DNA sequence of CTCL DNA for point mutations in *DNMT3A* and *ZEB1*.

a

Sample 14
CD28 p.F51V
Chr 2:20,4591,454
T → G

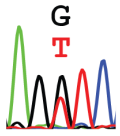

Sample 10
CD28 p.F51I
Chr 2:204,299,699
T → A

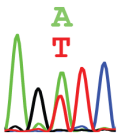

Sample 5
CD28 p.Q77P
Chr 2:204,299,699
C → A

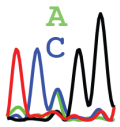

Sample 33
RHOA p.N117I
Chr3:49,474,991
T → A

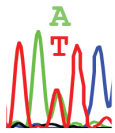

Sample 4
RHOA p.R70K
Chr3:49,380,933
C → T

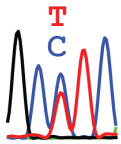

Sample 20
RHOA p.C16R
Chr 3:49,387,981
A → G

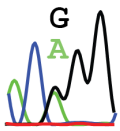

Gene	*CD28*			*RHOA*		
SSNV	F51V	F51I	Q77P	C16R	R70K	N117I
# samples with SSNV identified by exome sequencing	2	1	2	1	1	2
# samples with SSNV confirmed by Sanger sequencing	2	1	2	1	1	2

b

Sample 31
ZEB1 p.Y251C
Chr 10: 31,849,929
C → T

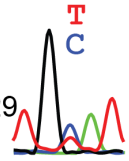

Sample 37
ZEB1 p.Q538*
Chr 10:31,849,929
C → T

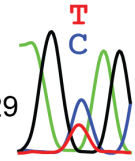

Sample 2
ZEB1 p.Q855*
Chr 10: 31,850,829
C → T

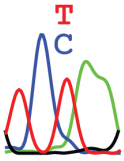

Sample 30
DNMT3A p.P233L
Chr 2: 25,324,567
G → A

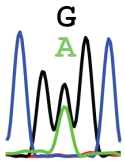

Sample 11
DNMT3A p.Y584*
Chr 2: 25,320,627
G → T

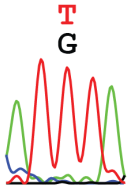

Sample 32
DNMT3A p.S669F
Chr 2: 25,318,011
G → A

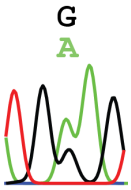

Sample 33
DNMT3A p.P777L
Chr 2: 25,315,581
G → A

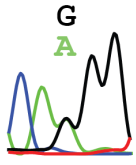

Gene	*DNMT3A*	*ZEB1*
# samples with SSNV identified by exome sequencing	4	3
# samples with SSNV confirmed by Sanger sequencing	4	3

Supplementary Figure 4. GISTIC 2.0 significance plots identifying recurrent focal SCNVs with a false discovery rate<0.25

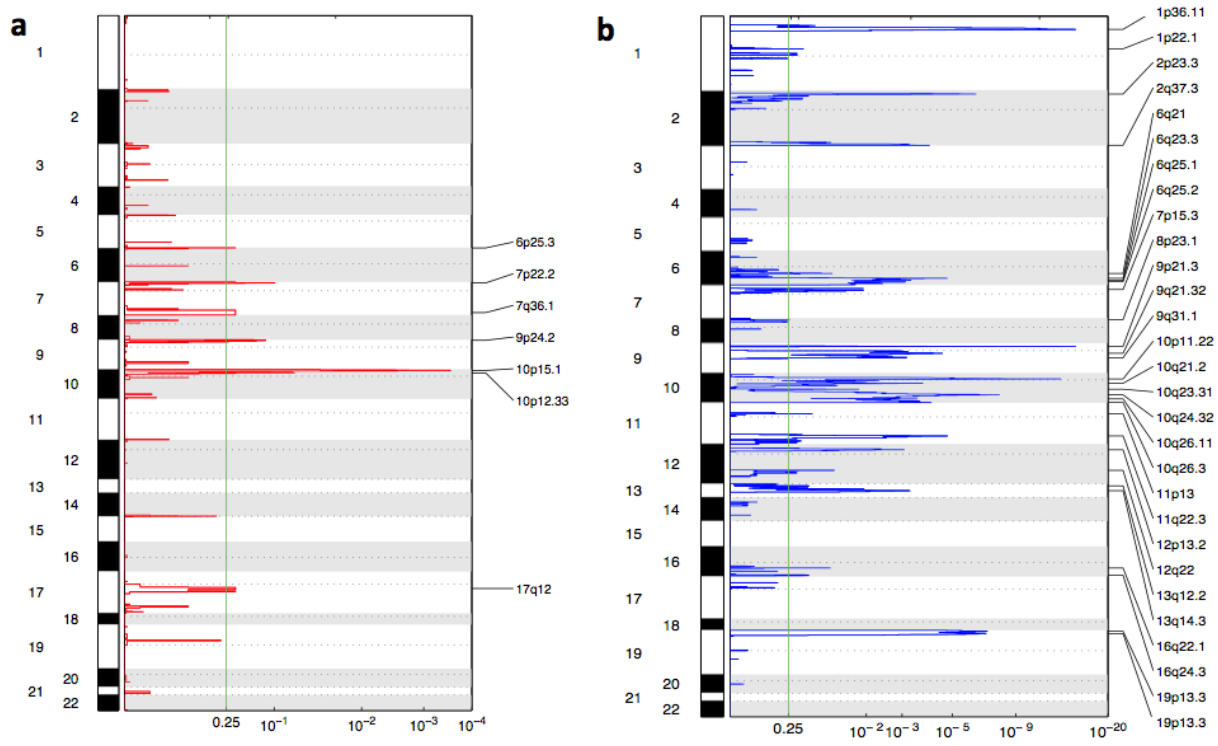

(a) GISTIC 2.0 plot identifying statistically significant recurrent amplifications. **(b)** GISTIC 2.0 plot identifying statistically significant recurrent deletions.

Supplementary Figure 5. Gene localizing mutations in significant SCNVs in CTCL.

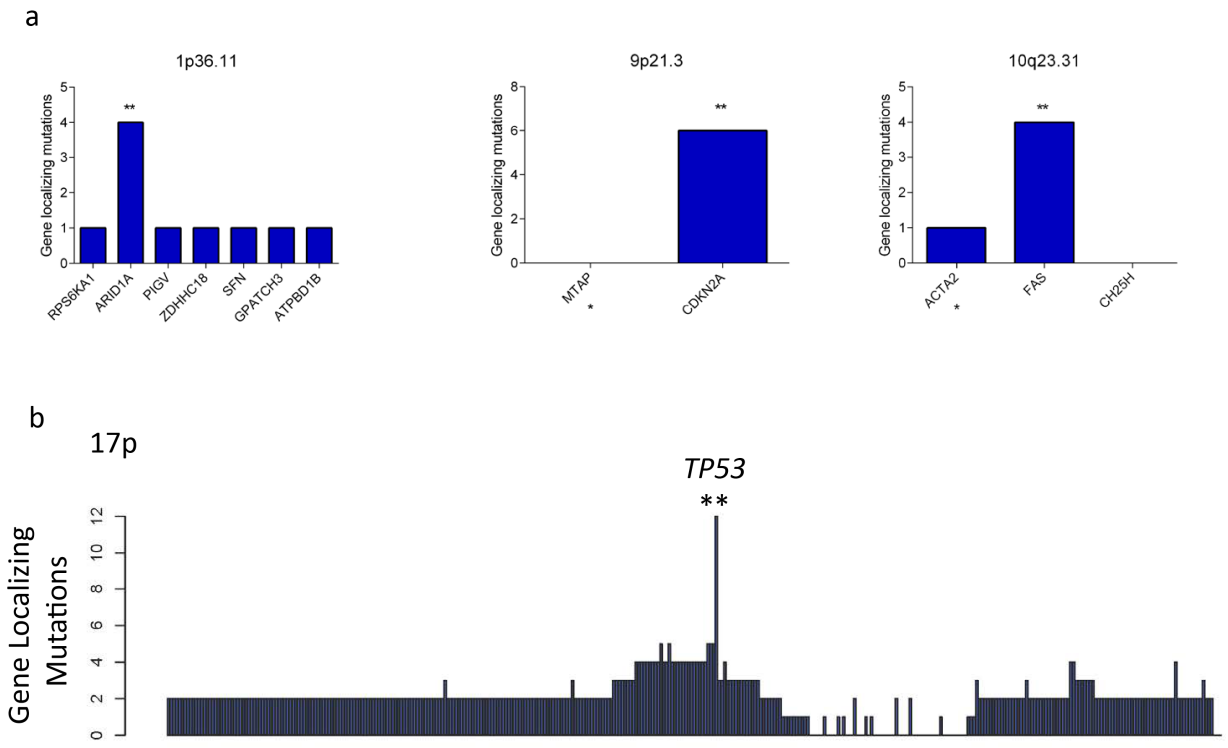

Gene localizing mutations for genes in **(a)** significant focal intervals or **(b)** significant arm-level events. Gene localizing mutations are defined as mutations that would affect at least one but not all genes in the interval. They include non-silent SSNVs and focal SCNVs that overlap with at least one but fewer than all genes in the interval. * indicates gene immediately outside of GISTIC interval. ** indicates likelihood of gene being the target gene in that interval >99.9%.

Supplementary Figure 6. Relative binding of wild-type CD28 or its mutants to CD80-Fc.

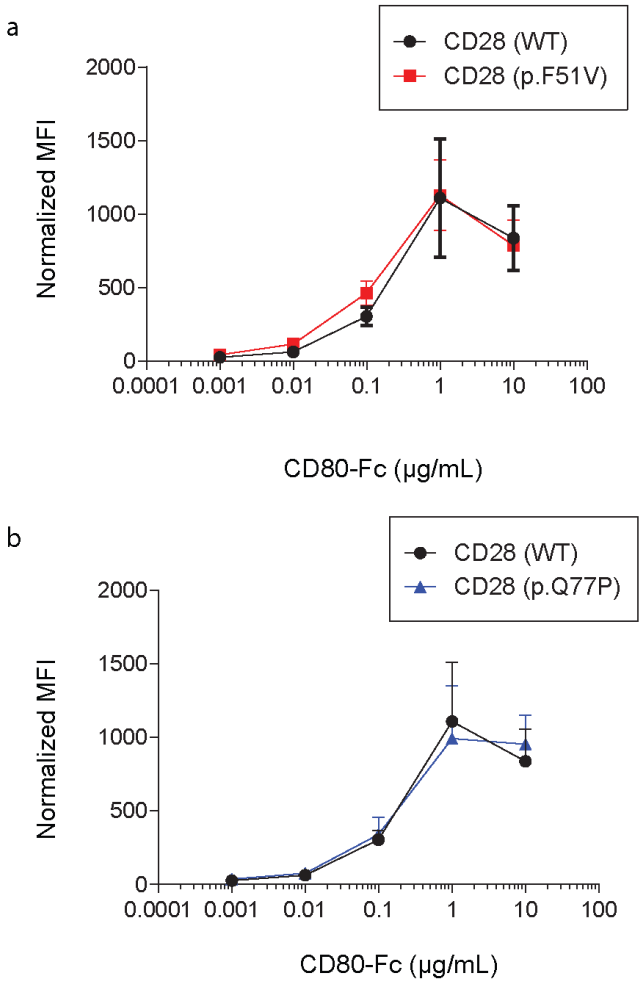

Aliquots of 293T cells expressing wild-type CD28 or its mutants (p.F51V (**a**) or p.Q77P (**b**)) were independently incubated with anti-CD28 antibody (eBioscience) or the indicated amounts of CD80-Fc (R&D Systems). CD80-binding was subsequently detected by Alexa Fluor 647-labeled secondary antibody (BD Pharmingen). Mean fluorescence intensity was determined from data histograms using FloJo. CD80-Fc binding was then normalized according to the relative expression of the CD28 isoform on the 293T cells. The graph plots normalized mean fluorescence intensity (MFI) as a function of CD80-Fc concentration. The results show the mean of three independent experiments with standard error.

Supplementary Figure 7. Relative CD86-Fc binding in cells expressing equivalent levels of CD28 isoforms.

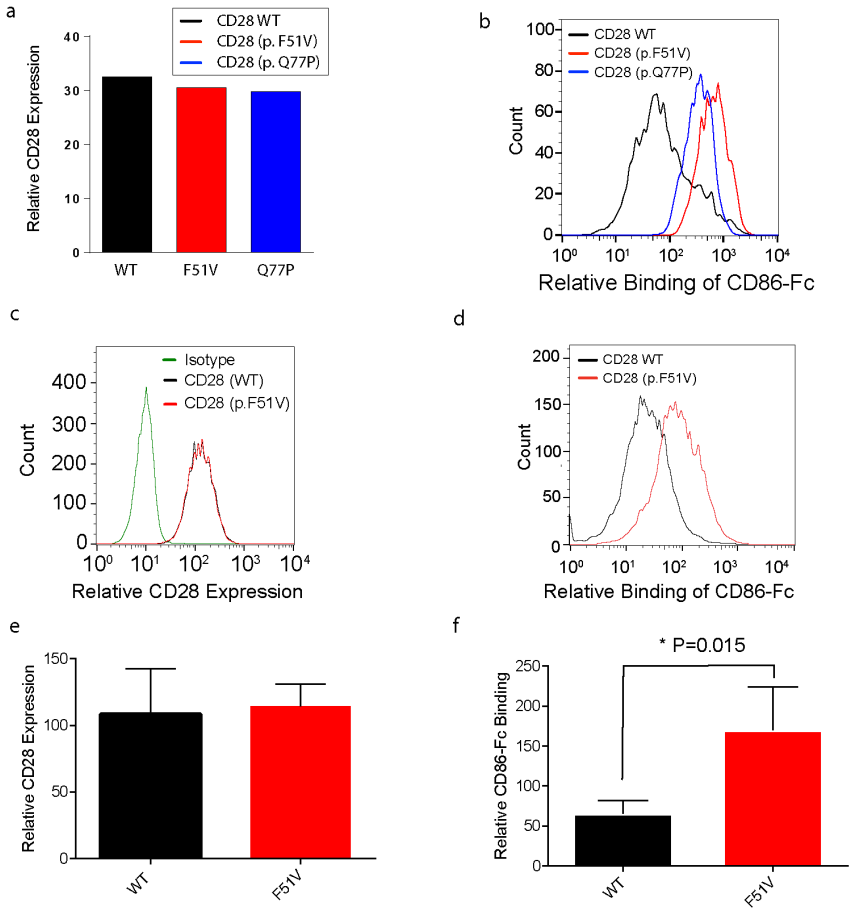

(a) 293T cells expressing wild-type (WT) CD28 or its mutants were simultaneously stained with both an anti-CD28 antibody (eBioscience) and CD86-Fc (R&D Systems). 293T cells were gated for equivalent levels of CD28 and the mean fluorescence intensity for each gated population is shown here. **(b)** Relative CD28 expression of gated 293T cells stably transduced with human WT CD28 or CD28 mutants (p.F51V or p.Q77P) (CD28 expression for this experiment is shown in (**a**)). CD28-expressing 293T cells were incubated with CD86-Fc (10 μg/ml), which was subsequently detected by Alexa Fluor 647-labeled secondary antibody (BD Pharmingen). **(c)** Relative expression of CD28 isoforms on Jurkat cells. In a representative experiment, Jurkat cells were stably transduced with WT CD28 or CD28 (p.Phe51Val) and stained with FITC-conjugated anti-CD28 antibody (eBioscience) or isotype control (Green). **(d)** FACS plots

demonstrating relative binding of CD86-Fc (10 μg/ml) to Jurkat cells expressing equivalent levels of WT CD28 or CD28 (p.Phe51Val). Relative CD28 expression for this experiment is shown in **(d)**. Binding of CD86-Fc was detected by Alexa Fluor 647-labeled secondary antibody. **(e)** Relative CD28 expression on Jurkat cells expressing human wild-type CD28 or its mutant (p.Phe51Val). The results show the mean of four biological replicates with standard error. (**f**) Relative binding of CD86-Fc (10 μg/ml) to Jurkat cells stably transduced with human wild-type CD28 or its mutant (p.Phe51Val). The relative CD28 expression for these experiments are shown in **(e).** The results show the mean of four biological replicates with standard error. * indicates $P<0.05$.

Supplementary Figure 8. Structural features of CTCL mutations in RHOA and PLCG1.

a

b

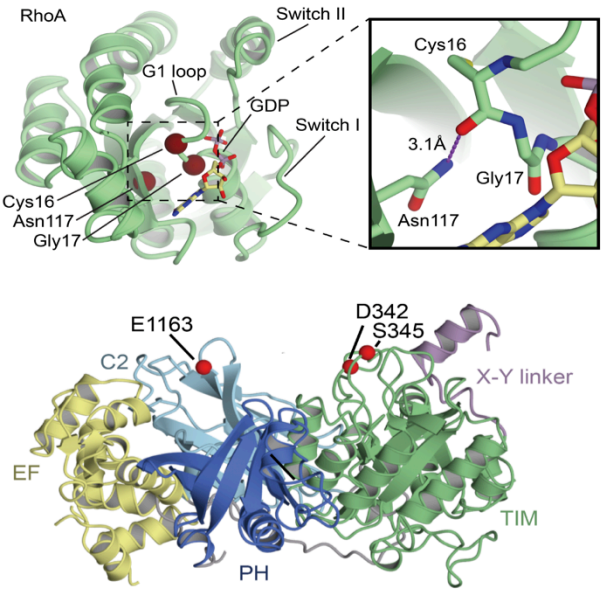

(a) Clustering of residues p.Cys16, p.Gly17 and p.Asn117 in the GTP binding pocket in RhoA. p.Gly17 and p.Asn117 are sites of recurrent mutations in T cell lymphoma that abolish RhoA's ability to bind GTP[1,2] (**Fig. 2a**). Crystal structure of RhoA in complex with GDP is shown (PDB ID: 1FTN)[3]. The tight clustering in the GTP binding pocket of residues p.Cys16, p.Gly17, and p.Asn117 are indicated. These amino acids are shown as red spheres. Inset shows the proximity of the three amino acids to the GDP molecule. The G1, Switch I and Switch II loops are indicated. **(b)** Clustering of residues of p.Asp342, p.Ser345 and p.Glu1163 on the surface of PLCG1 facing the plasma membrane. p.Ser345 has been previously shown to be a gain-of-function activating mutation in PLCG1[4]. p.Ser345 and p.Asp342 both cluster in the PLCx domain. These residues were mapped onto the crystal structure of PLCB2 (PDB ID 2ZKM)[5], a closely related member of the PLC isozyme family. Domains of PLCB2 are indicated. C2, C2 calcium binding domain; EF, EF-hand-domain pair; PH, Pleckstrin homology domain; TIM, catalytic TIM barrel; X-Y linker, linker region between Phospholipase C X and Phospholipase C Y domains. Figure generated using CCP4MG[6].

Supplementary Figure 9. Copy number plots of *NFKB2* in 3 samples with C-terminal truncating mutations.

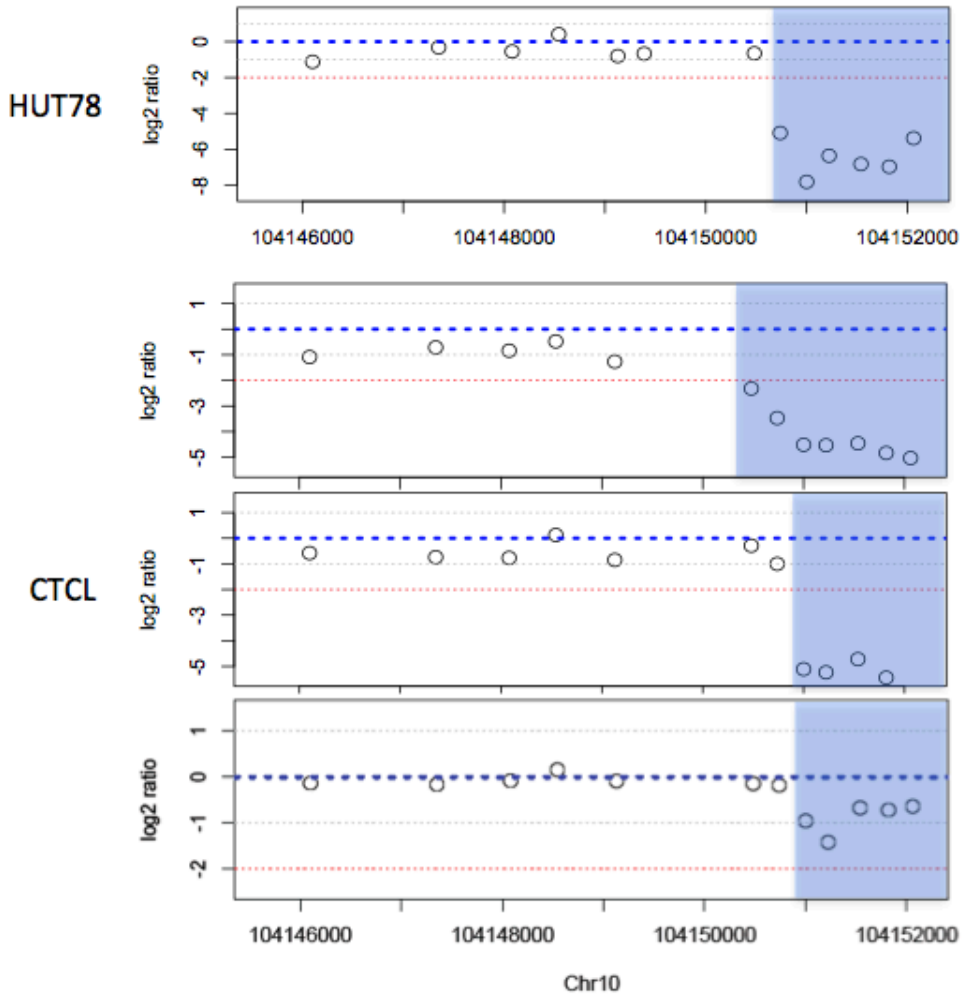

Log_2 relative ratio (log2 ratio) plots of *NFKB2* in 3 samples and Hut-78, a CTCL cell line with a known truncation in NFKB2. Each point represents a targeted region from the Nimblegen capture array. Intragenic deletions are indicated in blue.

Supplementary Figure 10. *TP53* and *ARID1A* deletions in CTCL.

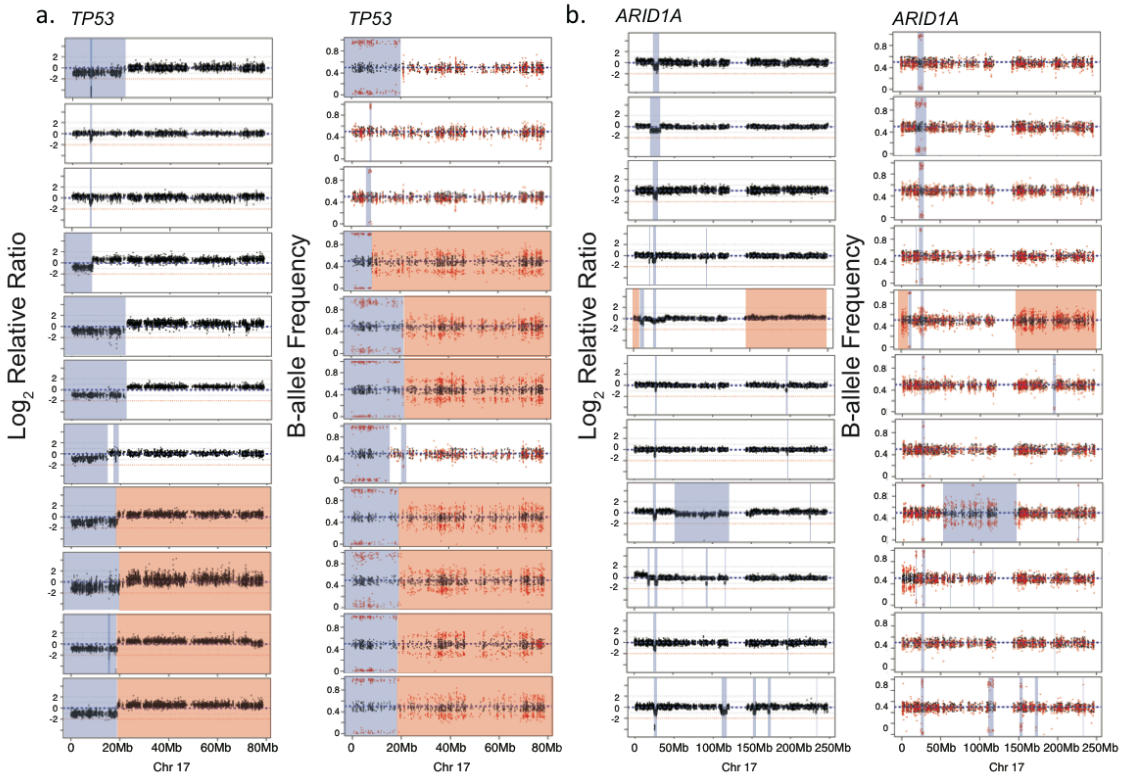

Representative $\log_2$ relative ratio and B-allele frequency plots of 11 samples with deletions in **(a)** *TP53* (chromosome17) and **(b)** *ARID1A* (chromosome 1). Deletions are shaded blue, and amplifications shaded in red.

Supplementary Figure 11. *DNMT3A* deletions in CTCL.

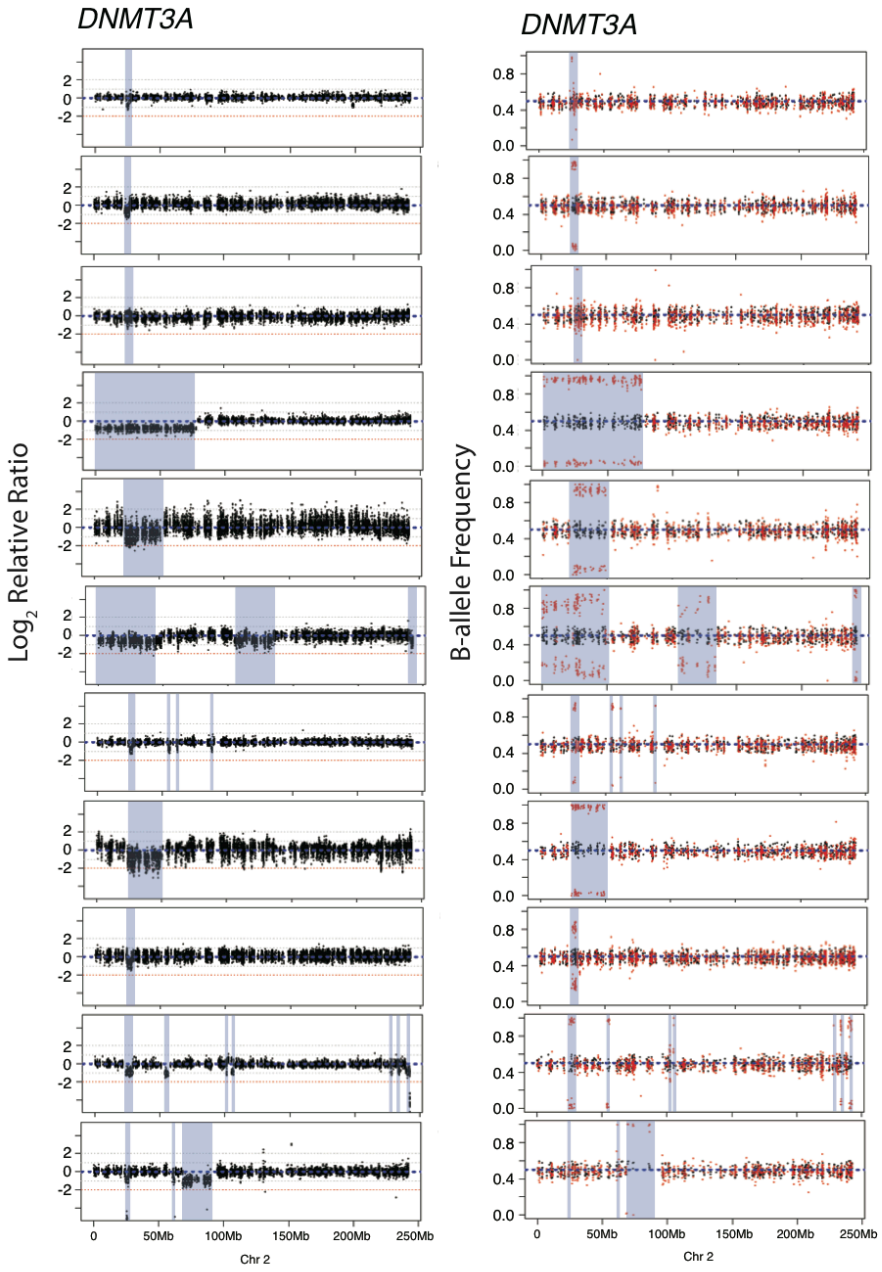

Representative $\log_2$ relative ratio and B-allele frequency plots of 11 samples with deletions in *DNMT3A* (chromosome 2).

Supplementary Figure 12. Loss of ZEB1 by shRNA increases GATA3 expression

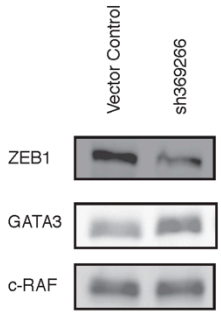

Western blots demonstrating the PMA/Ionomycin-induced expression of GATA3 in Jurkat cells transduced with pLKO vector control or pLKO targeting *ZEB1* (sh369266). C-RAF was used as a loading control.

Supplementary Figure 13. Resolution by whole genome sequencing of the breakpoints contributing to structural variants in CTCL.

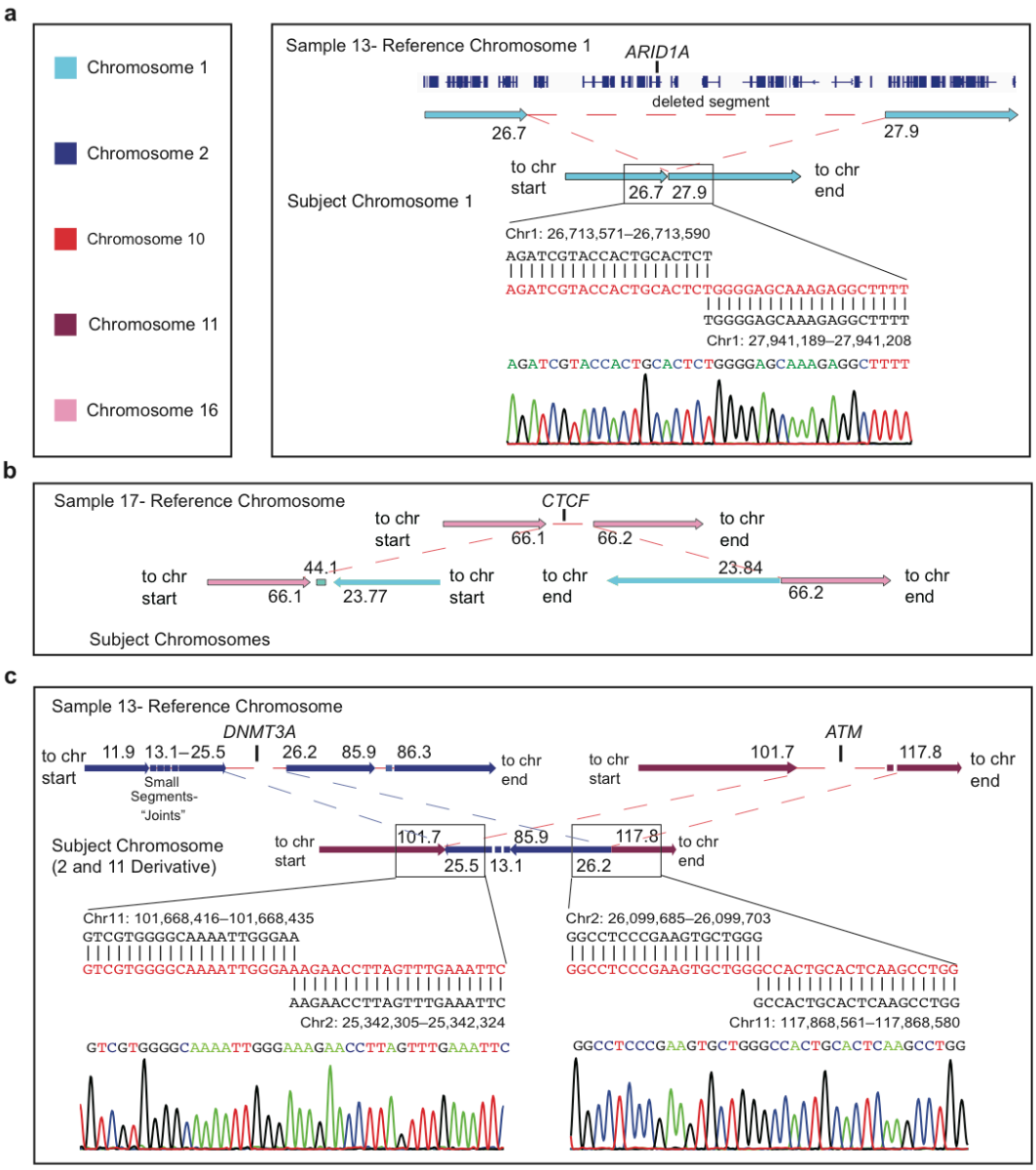

Structural variants leading to copy number loss of **(a)** *ARID1A*, **(b)** *CTCF*, and **(c)** *DNMT3A* and *ATM* elucidated by whole genome sequencing. Reference chromosomes reflect the wild-type chromosome. The dotted lines in the reference chromosome reference regions of genomic loss in CTCL. The subject chromosomes reflect the rearranged chromosome in the CTCL sample. Each arrow represents a contiguous chromosomal segment with directionality reflected by the arrowhead. The arrowhead

points in the direction of increasing nucleotide position number (hg18). Numbers listed are co-ordinates in hg18 (Mb). The numbers bordering each arrow reflects the nucleotide positions at closest breakpoint. Three breakpoints were confirmed by Sanger DNA sequencing.

Supplementary Figure 14. Resolution by whole genome sequencing of the breakpoints contributing to significant structural variants on chromosome 10

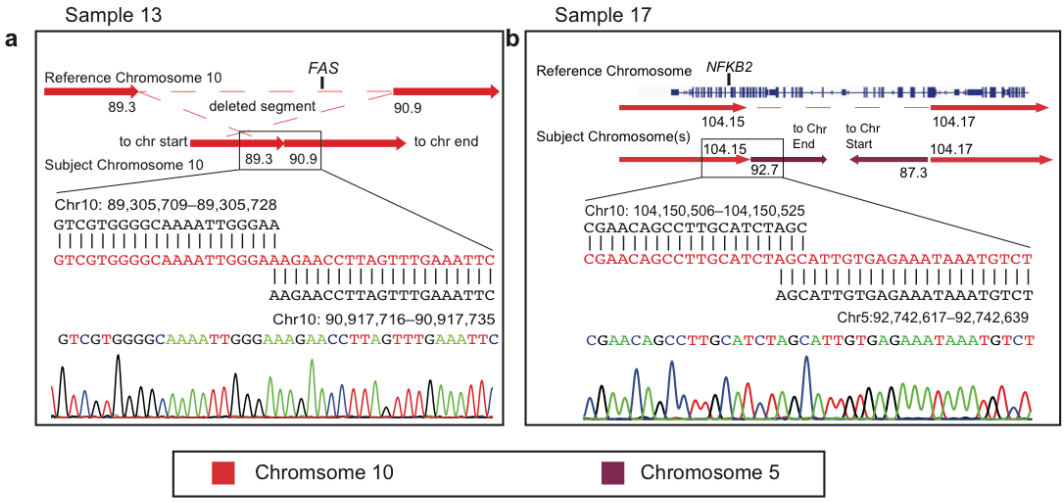

Structural variants leading to **(a)** copy number loss of *FAS*, **(b)** C-terminal truncation of *NFKB2*. Reference chromosomes reflect the wild-type chromosome. The dotted lines in the reference chromosome represent regions of genomic loss in CTCL. The subject chromosomes reflect the rearranged chromosome in the CTCL sample.

Each arrow represents a contiguous chromosomal segment with directionality reflected by the arrowhead. The arrowhead points in the direction of increasing nucleotide position number (hg18). Numbers listed are co-ordinates in hg18 (Mb). The numbers bordering each arrow reflects the nucleotide positions at closest breakpoint. Two breakpoints were confirmed by Sanger DNA sequencing.

Supplementary Figure 15. Chromothripsis-like complex genomic rearrangements in CTCL.

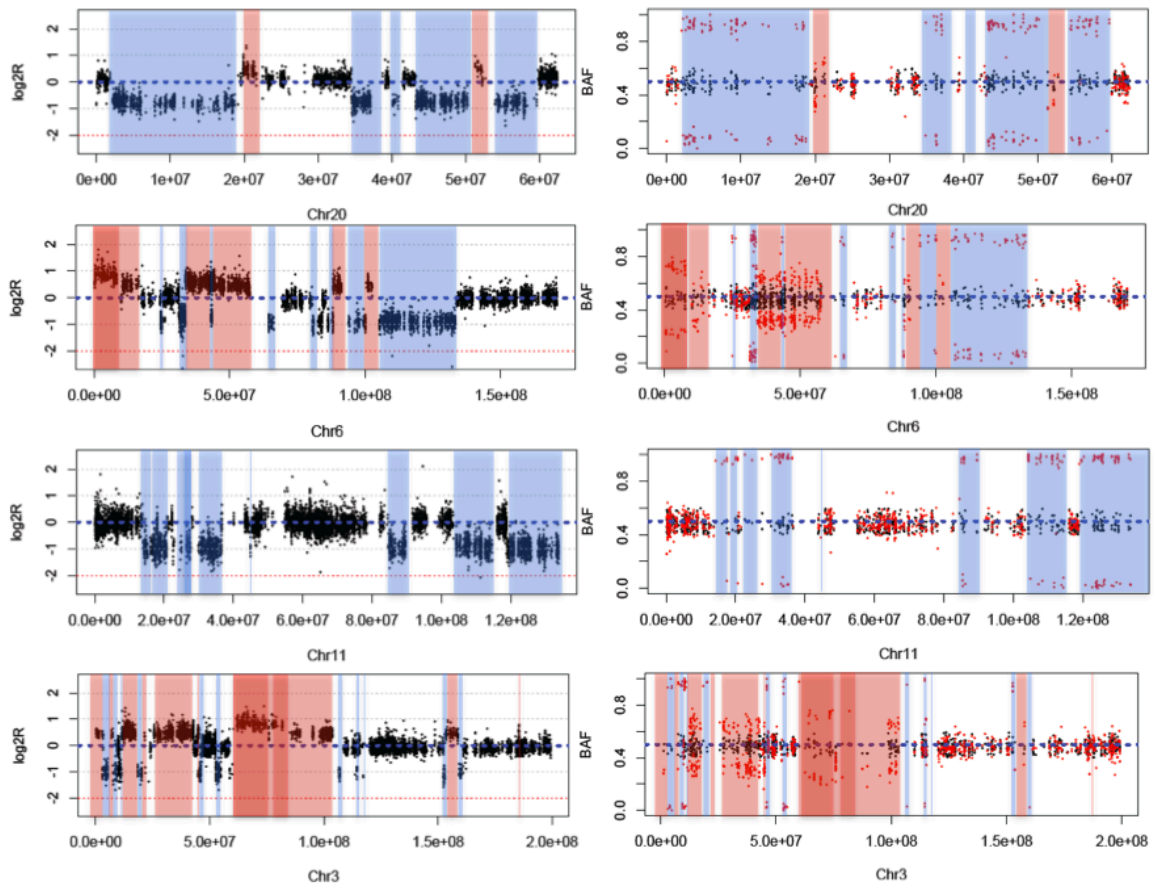

Log_2 relative ratio (log2R) and B-allele frequency (BAF) plots of 4 select chromosomes with >10 SCNVs.

Supplementary Figure 16. Enrichment of high scoring RAG heptamers at CTCL breakpoints.

a

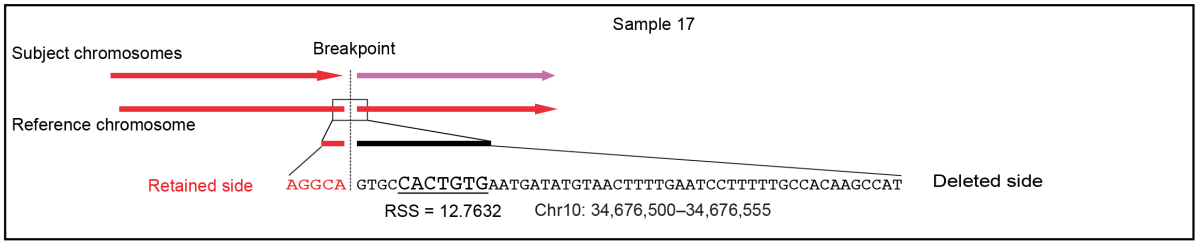

b

Cancer Type	Total Breakpoints	Total breakpoint windows with high scoring heptamers	Prevalence of high scoring heptamers in breakpoint windows	P-value
CTCL	102	13	12.7%	-
Gastric	24,046	1,612	6.7%	0.019
Melanoma	3,421	259	7.6%	0.048
Pancreatic	754	52	6.9%	0.035
Prostate	4,301	272	6.3%	0.014

c

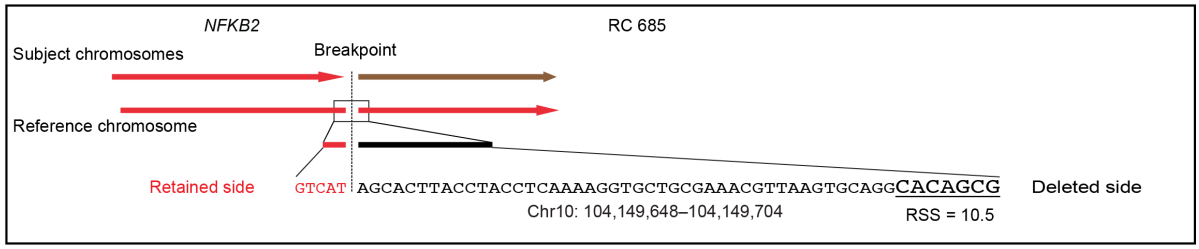

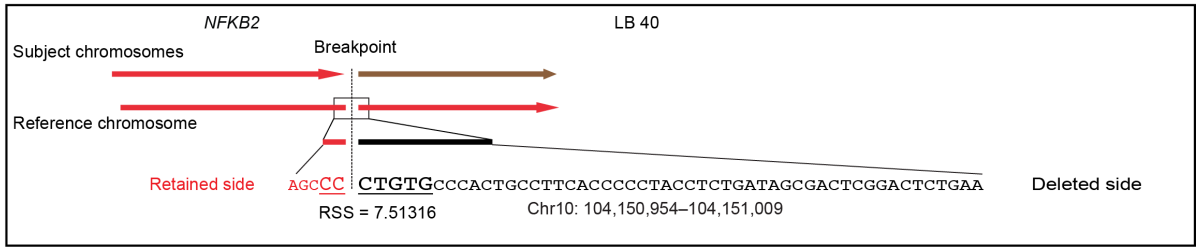

(a) Schematic of the 55 bp breakpoint window which was used to identify high scoring heptamers including 5 bp of the retained DNA and up to 50 bp of the deleted DNA. A high scoring heptamer with strong homology to RAG consensus cleavage sites (RSS>8.55) is underlined. (**b**) Table of frequency of high scoring RAG heptamers in in the breakpoint window of CTCL and other cancers. The prevalence of heptamers in the breakpoint window was compared between CTCL and other cancer types. P-value was established using one-sided Fisher's test. (**c**) Identification of high-scoring heptamers

(RSS>7.5) in the 55 bp window at the published breakpoints of oncogenic NFKB2 C-terminal truncations of two B-cell lymphomas (RC655, LB40)[7].

Supplementary Figure 17. RSS scores of heptamers in the endogenous human TCR loci.

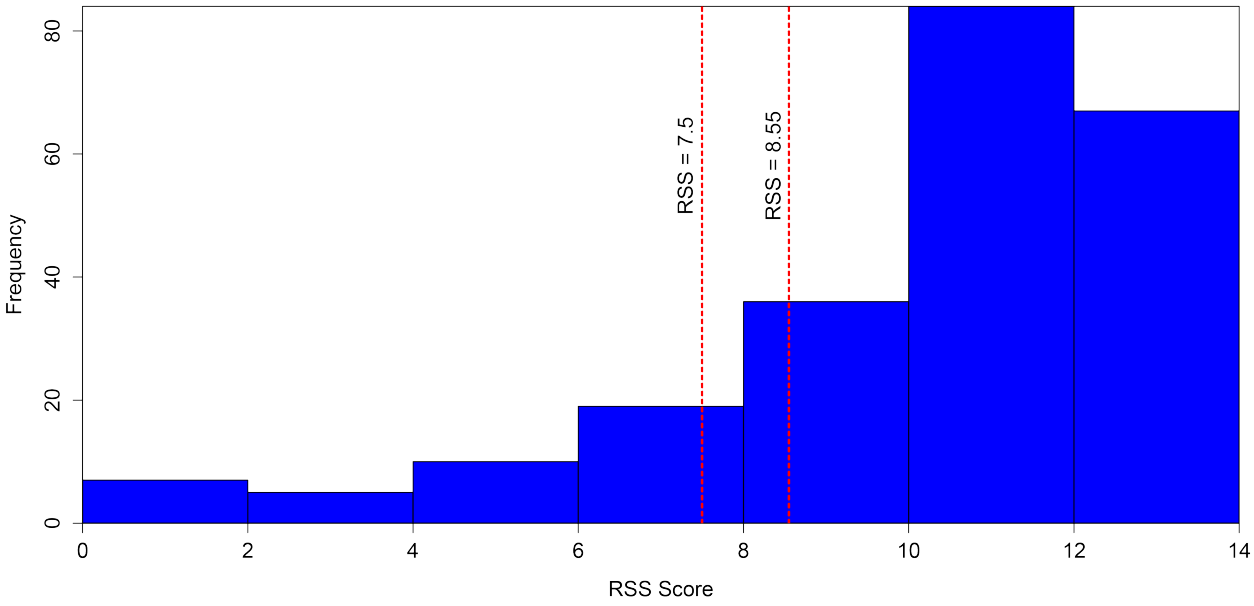

RAG signal sequences at the endogenous human T cell receptor gene loci were obtained from RSSsite[10]. The heptamers at the recombination signal sequences were assessed for similarities to the consensus sequence (CACAGTG) using FIMO[11]. 31 of 228 heptamers at RSS sites (13.6%) had an RSS score between 7.5 and 8.55.

References for Supplementary Information:

1. Sakata-Yanagimoto, M. *et al.* Somatic RHOA mutation in angioimmunoblastic T cell lymphoma. *Nat Genet* **46**, 171-5 (2014).
2. Khosravi-Far, R., Solski, P.A., Clark, G.J., Kinch, M.S. & Der, C.J. Activation of Rac1, RhoA, and mitogen-activated protein kinases is required for Ras transformation. *Mol Cell Biol* **15**, 6443-53 (1995).
3. Wei, Y. *et al.* Crystal structure of RhoA-GDP and its functional implications. *Nat Struct Biol* **4**, 699-703 (1997).
4. Vaque, J.P. *et al.* PLCG1 mutations in cutaneous T-cell lymphomas. *Blood* (2014).
5. Hicks, S.N. *et al.* General and versatile autoinhibition of PLC isozymes. *Mol Cell* **31**, 383-94 (2008).
6. McNicholas, S., Potterton, E., Wilson, K.S. & Noble, M.E. Presenting your structures: the CCP4mg molecular-graphics software. *Acta Crystallogr D Biol Crystallogr* **67**, 386-94 (2011).
7. Neri, A., Fracchiolla, N.S., Migliazza, A., Trecca, D. & Lombardi, L. The involvement of the candidate proto-oncogene NFKB2/lyt-10 in lymphoid malignancies. *Leuk Lymphoma* **23**, 43-8 (1996).